

of olivine differ somewhat but not greatly from the present bronzite data, except in the value of $(\partial K^T/\partial P)_T$, for which a difference of a factor of about 2 occurs. Because the Fe/Mg ratio in both materials is approximately the same, this difference is attributed to the different crystal structures. Although the composition of the garnet specimen differs considerably from the compositions of the bronzite and olivine samples (it corresponds to an almandine to pyrope ratio of about 3:1), the pressure coefficients of the bulk modulus and of the shear modulus are closer to the values for the olivine sample. The contrast with the bronzite data underlines again the unusual properties of the enstatite structure.

It is important to note that, from the compression data of Bridgman [1948] on hypersthene, an equally large value for the isothermal first pressure derivative of the bulk modulus is obtained. Bridgman's data are expressed in the form $(V_0 - V)/V = aP + bP^2$, where V_0 and V are the specimen volumes at ambient and elevated pressures, respectively, $a = 1.08 \text{ Mb}^{-1}$, $b = 5.2 \text{ Mb}^{-2}$, and $\rho_0 = 3.42 \text{ g/cm}^3$ for the hypersthene sample studied. The isothermal bulk modulus and its isothermal pressure derivative are obtained from the relations [Anderson, 1966] $K^T = 1/a = 0.9259 \text{ Mb}$ and $(\partial K^T/\partial P)_T = 2b(K^T) - 1 = 7.9$. Although Bridgman's data are less accurate than the present acoustic data, the large value of $(\partial K^T/\partial P)_T$ obtained from his measurements is indicative of the anomalous behavior of orthopyroxene at high pressure.

Incomplete velocity measurements as a function of temperature and pressure have also been performed on natural rock specimens containing primarily bronzite [Hughes and Nishitake, 1963; Birch, 1960; Simmons, 1964]. These data have been combined by Anderson and Sammis [1970] to give the complete set of data of the velocities and their derivatives with respect to temperature and pressure (Table 13). The results calculated from the present single-crystal data by means of the VRH average are also shown for comparison. Although, because of porosity, heterogeneity, and grain size, the accuracy of data from natural rock specimens is usually not very good, the two sets of data shown in Table 13 are in fair agreement.

Nonlinearity of pressure dependence. In Figure 6 the pressure dependence of the on-diagonal shear moduli is plotted as calculated from the

TABLE 13. Comparison of Present Bulk Velocity Data Obtained by Using VRH Averages with Those Measured in Bronzite Rock Samples

Parameter	Present Data	Anderson and Sammis [1970]*
ρ , g/cm ³	3.354	3.279
V_P , km/sec	7.78	7.64
V_S , km/sec	4.72	5.59
$(\partial V_P/\partial P)_T$, 10 ⁻³ km/sec kb	20.57	19.00
$(\partial V_P/\partial T)_P$, 10 ⁻⁴ km/sec °C	-9.08	-6.40
$(\partial V_S/\partial P)_T$, 10 ⁻³ km/sec kb	5.16	7.00
$(\partial V_S/\partial T)_P$, 10 ⁻⁴ km/sec °C	-4.86	-6.00

*Based on data from Hughes and Nishitake [1963], Birch [1960], and Simmons [1964].

measured elastic data according to the linear approximation

$$c_{\mu\nu} = c_{\mu\nu}^0 + (\partial c_{\mu\nu}/\partial P)_0 P \quad (10)$$

and according to the quadratic approximation

$$c_{\mu\nu} = c_{\mu\nu}^0 + (\partial c_{\mu\nu}/\partial P)_0 P + (\partial^2 c_{\mu\nu}/\partial P^2)_0 (P^2/2) \quad (11)$$

It is apparent that, at pressures above about 20–30 kb, considerable deviations from the linear relation (10) arise as a result of the quadratic term in (11) and that, for c_{11} and c_{33} , maximums occur at about 85 and 50 kb, respectively. Without knowledge of the derivatives higher than second order or of the convergence of the Taylor expansion of the elastic constants with respect to pressure or both, it is, of course, not possible to establish the exact functional dependence on pressure in the range considered. Because calculations for alkali halides based on model potentials show that the exact pressure dependence falls between the linear dependence and the quadratic dependence [Barsch and Shull, 1971], it is not unreasonable to expect qualitatively similar behavior for bronzite. Thus for two of the three on-diagonal shear moduli a substantial deviation from nonlinearity would remain, even if the quadratic terms would be reduced, for example, to half their values.

The remaining shear moduli are functions of the on-diagonal longitudinal moduli c_{11} , c_{22} , and c_{33} , of the cross-coupling moduli c_{12} , c_{13} , and c_{23} , and of the direction cosines of the propagation direction. Because it was not possible to measure the second pressure derivatives of the on-diagonal

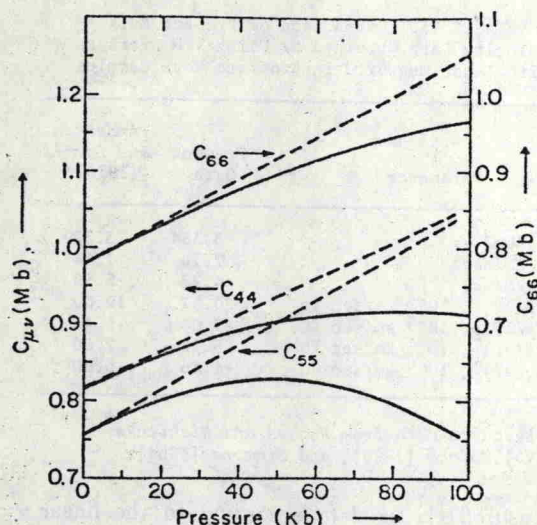


Fig. 6. Pressure dependence of on-diagonal shear constants. Dashed lines indicate linear extrapolation; solid lines, quadratic extrapolation.

longitudinal moduli, the second pressure derivatives of these shear moduli are still unknown. However, because the nonlinearity found for the quasi-shear modes (see, for example, the curve for $N \parallel [10\bar{n}]$ and $U \parallel [n0\bar{l}]$ in Figure 3) and the second pressure derivatives of the cross-coupling moduli determined from the assumption $(\partial^2 c_{\mu\nu}/\partial P^2) = 0$ ($\mu = 1, 2, 3$, no summation) (Table 6) are of the same order of magnitude as those of the on-diagonal shear moduli, it is to be expected that the second pressure derivatives of the remaining shear moduli are of the same order of magnitude. By the same token, the second pressure derivatives of the isotropic shear modulus, which depend in the VRH approximation on the second pressure derivatives of all nine elastic constants, should be expected to be roughly equal to the average of the second pressure derivatives of the on-diagonal shear moduli (approximately -33 Mb^{-1}). In connection with the values of the isotropic shear modulus (0.75 Mb) and its first pressure derivative (2.38), it is thus apparent that, at the highest pressures of the stability range of orthopyroxene (about 90–135 kb [Ringwood, 1967; Akimoto and Syono, 1970; Ahrens and Gaffney, 1971]), small deviations for a nonlinear pressure dependence may become noticeable and should be included in accurate geophysical applications.

To compare the magnitude of the second pressure derivatives of the elastic constants with

the corresponding values of other materials, it is convenient to consider the dimensionless quantity $K^T(\partial^2 c_{\mu\nu}/\partial P^2)$. With $K^T = 0.988 \text{ Mb}$ and the data of Table 8, this quantity is seen to range from -14 to -57 for the three on-diagonal shear moduli. For the eight alkali halides for which the second pressure derivatives of the elastic constants have been measured and which represent both the rocksalt and the cesium chloride structures, the quantity $K^T(\partial^2 c_{\mu\nu}/\partial P^2)$ ranges from -1 to -4.5 [Chang and Barsch, 1967, 1971; Barsch and Shull, 1971]. For spinel a value of -5.5 has been measured [Chang and Barsch, 1972]. Thus the values reported here for bronzite appear to be anomalously large. An explanation of this behavior requires a lattice theoretical analysis based on the crystal structure of enstatite, similar to the analysis presented for spinel by Striefler and Barsch [1972]. Although such an analysis is not yet available, it appears plausible to attribute the large curvature to the phase transition or the disproportionation of enstatite between about 90 and 135 kb [Akimoto and Syono, 1970; Ahrens and Gaffney, 1971]. The decrease of the shear moduli at pressures above the maximums displayed in Figure 6 indicates decreasing mechanical stability paralleled by decreasing thermodynamic stability and the occurrence of a phase transformation before the mechanical stability limit (e.g., if the quadratic extrapolation is used, $c_{33} = 0$ at $P \approx 220 \text{ kb}$) is reached.

Compression of bronzite at very high pressures. The ultrasonic equation of state has been calculated from the present bronzite data by using the first-order Birch equation (Figure 7). For illustrative purposes only, the nonlinear elastic data for bronzite have also been extrapolated by using the second-order Birch equation of state. These data are also included in Figure 7. Although the nonlinear data are quite uncertain, it is interesting to note that the deviation from the linearly extrapolated data is quite small at 150 kb. If geophysical applications where temperature effects are important to depths of $>200 \text{ km}$ are considered, it is unlikely that this small difference caused by the curvature will play an important role in the equation of state. This conclusion is no longer valid, of course, if the orthopyroxene-garnet transition does not occur and the stability